

Spin dynamics in the electron-doped Kondo insulator $\text{Yb}_{1-x}\text{Zr}_x\text{B}_{12}$ ($x=0.2$)K. S. Nemkovski,¹ P. A. Alekseev,¹ J.-M. Mignot,² E. A. Goremychkin,^{3,4} A. A. Nikonov,¹ O. E. Parfenov,¹ V. N. Lazukov,¹ N. Yu. Shitsevalova,⁵ and A. V. Dukhnenko⁵¹RRC “Kurchatov Institute,” Kurchatov sq. 1, 123182 Moscow, Russia²Laboratoire Léon Brillouin, CEA/Saclay, CEA-CNRS, 91191 Gif sur Yvette, France³Materials Science Division, Argonne National Laboratory, Argonne, Illinois 60439-4845, USA⁴ISIS Pulsed Neutron and Muon Facility, Rutherford Appleton Laboratory, Chilton, Didcot OX11 0QX, United Kingdom⁵Institute for Problems of Materials Science, NASU, Kiev, Ukraine

(Received 23 December 2009; revised manuscript received 5 February 2010; published 8 March 2010)

Electron doping of the Kondo insulator YbB_{12} has been achieved by substitution of tetravalent Zr in the newly synthesized $\text{Yb}_{0.8}\text{Zr}_{0.2}\text{B}_{12}$ solid solution. Neutron-scattering measurements of the spin dynamics are reported, together with electrical resistivity and ac magnetic-susceptibility data. Zr doping transforms the spin-gap spectral response into a pseudogap shape and makes its temperature evolution much smoother than in the $\text{Yb}_{1-x}\text{Lu}_x\text{B}_{12}$ family studied previously. The results obtained are discussed in connection with the local bound-state picture for the Kondo insulator.

DOI: [10.1103/PhysRevB.81.125108](https://doi.org/10.1103/PhysRevB.81.125108)

PACS number(s): 71.70.Ch, 75.30.Mb, 75.40.Gb, 78.70.Nx

I. INTRODUCTION

YbB_{12} is an example case of a strongly correlated electron system exhibiting Kondo insulator (KI) behavior at low temperature.¹ This peculiar regime, achieved on cooling below $T^* \sim 50$ K,² is characterized by the opening of a narrow gap in the electronic density of states and the quenching of local-moment paramagnetism, ascribed to a singlet ground-state formation. In spite of intensive investigations, the nature of this nonmagnetic semiconducting state remains a subject of debate.³⁻⁵ We have previously reported a detailed inelastic neutron-scattering (INS) study of spin dynamics in pure YbB_{12} , as well as in a series of $\text{Yb}_{1-x}\text{Lu}_x\text{B}_{12}$ solid solutions where nonmagnetic “defects” are introduced in the magnetic sublattice.⁶⁻⁸ It was found that, in both cases, the magnetic excitation spectrum at low temperature is characterized by a spin gap and, close to the gap edge, three well-defined dispersive excitations (denoted $M1$, $M2$, and $M3$) centered around 15, 20, and 40 meV, respectively. On increasing temperature above T^* , the spin gap is rapidly filled up by a broad quasielastic (QE) signal. In the same temperature range, the excitations $M1$, $M2$, and $M3$ are gradually suppressed whereas a new q -independent spectral component (M_h) appears at $E \approx 23$ meV.

The most widely used model describing the ground state in KIs is based on a hybridization mechanism between the conduction band and a narrow f -electron band.⁹ However, we have shown from experiments on diluted samples $\text{Yb}_{1-x}\text{Lu}_x\text{B}_{12}$ ($x=0.25-0.9$) (Refs. 10 and 11) that the spin gap (and, therefore, the singlet ground state) are not suppressed when the periodicity of the rare-earth (RE) sublattice is disrupted by Lu substitution. This behavior is difficult to reconcile with the latter (coherent) hybridization gap picture, and single-site scenarios, as proposed by Kasuya,¹² Liu,¹³ or Barabanov and Maksimov,⁵ may prove more realistic. Along this line, the semiconducting singlet ground state can be roughly described as the local bound state formed by one f hole [Yb^{3+} has a $4f^{13}$ configuration] and one conduction (d) electron with antiparallel spins. The gap value then corre-

sponds to the energy needed to dissociate this f - d bound state, and the $M2$ and $M3$ excitations⁸ to transitions from the singlet ground state to the lowest $4f^{13}$ spin-orbit multiplet states ($^2F_{7/2}$) split by a residual crystal-field (CF) effect. As to the low-energy excitation $M1$, it was interpreted⁷ as a spin exciton formed within the spin gap as a result of strong dynamical antiferromagnetic correlations between Yb sites. On the other hand, high-temperature spectra could be explained⁸ in terms of the Yb^{3+} CF scheme, strongly renormalized by f - d hybridization as previously observed in classical heavy-fermion compounds.

The above single-site picture assumes a central role of d -electron states at the RE sites in the formation of the KI ground state. To test this idea, it seems promising to study systems in which Yb is replaced by another atom with a different structure and occupancy of its d shell. This can be achieved through the partial substitution of Yb by Zr. Zr disturbs the YbB_{12} conduction band in two ways: (i) it contributes $4d$ electrons instead of $5d$ electrons and (ii) in dodecaborides, Zr is tetravalent whereas Yb and Lu are trivalent, thus supplying one extra electron to the conduction band. In this work, we have synthesized $\text{Yb}_x\text{Zr}_{1-x}\text{B}_{12}$ solid solutions, and characterized them by electrical resistivity and magnetic-susceptibility experiments. Spin-dynamics measurements performed in the compound with 20% Zr substitution reveal significant differences with respect to the previous Lu substitution results, lending further support to the above “ f - d bound-state” picture.

II. EXPERIMENTS

Powder with composition $\text{Yb}_{0.8}\text{Zr}_{0.2}\text{B}_{12}$ was synthesized at the Institute for Problems of Materials Science in Kiev by borothermal reduction from a mixture of ytterbium and zirconium oxides. ¹¹B isotope (99.5% enrichment) was used in order to reduce neutron absorption. The material was subsequently remelted using the traveling-solvent floating-zone technique, then powdered and etched with nitric acid ($\text{HNO}_3:\text{H}_2\text{O}=1:1$) to remove the YbB_6 phase. X-ray dif-

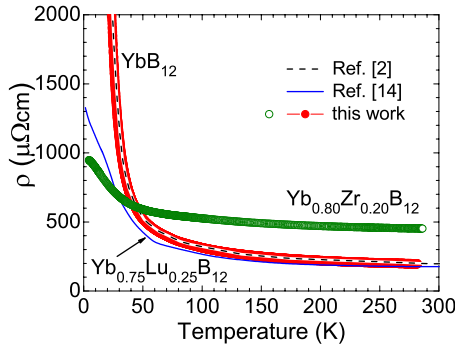


FIG. 1. (Color online) Temperature dependence of the electrical resistivities of $\text{Yb}_{0.8}\text{Zr}_{0.2}\text{B}_{12}$ and YbB_{12} , normalized at $T=300$ K to the value obtained in Ref. 2 for single-crystal YbB_{12} (see text). The results from Ref. 2 are shown by the dotted line. Also displayed are data for $\text{Yb}_{0.75}\text{Lu}_{0.25}\text{B}_{12}$ from Ref. 14.

fraction measurements confirmed the compound to have the expected face-centered-cubic structure and lattice parameter, $a=7.4561(4)$ Å. Phase analysis revealed traces of YbB_6 and, possibly, of some boron-rich phases (YbB_{28} or YbB_{66}). The full-profile Rietveld analysis indicates that Zr atoms are located at RE positions, and that the sample obtained does correspond to the composition $x=0.20\pm 0.04$. This value is in a good agreement with that obtained from the interpolation of the lattice parameter between YbB_{12} and ZrB_{12} values [7.4684(3) and 7.4077(9) Å, respectively] using Vegard's law. The same YbB_{12} sample previously studied in Ref. 6 was used here for the magnetic and transport measurements.

Electrical resistivity measurements were performed by the standard four-lead technique in the temperature range 4.2–285 K. The ac magnetic susceptibility was measured from 4.2 to 350 K in a weak magnetic field with average magnitude of about 15 Oe at frequencies comprised between 1 and 20 Hz.

INS experiment was carried out on the time-of-flight spectrometer HET at ISIS/RAL (U.K.) using a closed-cycle refrigerator ($4.5\leq T\leq 250$ K). Most measurements were performed at an incident neutron energy of $E_i=80$ meV. Under such conditions, a flat sample of 8.24 g, with a thickness of ~ 3 mm has a quite acceptable transmission coefficient of 70%. At two temperatures (4.5 and 150 K), spectra were also measured with a higher resolution, using $E_i=40$ meV and $E_i=20$ meV. A LuB_{12} specimen was used to estimate the nonmagnetic background. Absolute calibration of the spectral data was achieved by normalization to a vanadium standard.

III. RESULTS AND DISCUSSION

The electrical resistivities of $\text{Yb}_{0.8}\text{Zr}_{0.2}\text{B}_{12}$ and YbB_{12} are presented in Fig. 1. The true geometrical factor for pressed powder samples is not well defined, and the specific resistivity thus cannot be obtained directly from the raw data. However, by normalizing the resistance of YbB_{12} at $T=300$ K to the single-crystal resistivity value from Ref. 2, one notes the excellent agreement between the two data sets in the temperature range $20\leq T\leq 300$ K, indicating that the tempera-

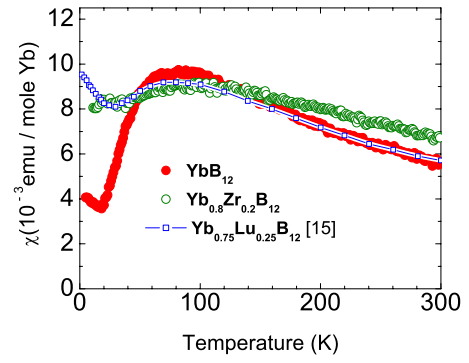


FIG. 2. (Color online) Temperature dependence of the bulk ac magnetic susceptibilities of $\text{Yb}_{0.8}\text{Zr}_{0.2}\text{B}_{12}$, YbB_{12} , and $\text{Yb}_{0.75}\text{Lu}_{0.25}\text{B}_{12}$ (Ref. 15).

ture dependences of the resistivities are closely similar for both materials. The YbB_{12} and $\text{Yb}_{0.8}\text{Zr}_{0.2}\text{B}_{12}$ slabs used in the present experiments were prepared under identical conditions and had very similar dimensions. Therefore, one can get a reasonable estimate of the $\text{Yb}_{0.8}\text{Zr}_{0.2}\text{B}_{12}$ resistivity by assuming that their geometrical factors are approximately equal. This leads to a room-temperature resistivity for $\text{Yb}_{0.8}\text{Zr}_{0.2}\text{B}_{12}$ which is significantly higher than in YbB_{12} . This may reflect a change in the electron band structure of $\text{Yb}_{0.8}\text{Zr}_{0.2}\text{B}_{12}$ as compared to the pure compound. In YbB_{12} , the resistivity exhibits an activation behavior characteristic of Kondo insulators.¹ The gap energy $E_a\sim 55$ K is close to the literature value² $E_a=68$ K (the difference being due to a small deviation occurring below 20 K). In $\text{Yb}_{0.8}\text{Zr}_{0.2}\text{B}_{12}$, an activation behavior is also observed in the range $30<T<100$ K but E_a is reduced to about 20 K, which is qualitatively similar to the effect of dilution by Lu. The resistivity of $\text{Yb}_{0.75}\text{Lu}_{0.25}\text{B}_{12}$ from Ref. 14 is also plotted in Fig. 1 for comparison.

The magnetic susceptibilities measured for $\text{Yb}_{0.8}\text{Zr}_{0.2}\text{B}_{12}$, YbB_{12} , and $\text{Yb}_{0.75}\text{Lu}_{0.25}\text{B}_{12}$ (Ref. 15) are shown in Fig. 2. The $\chi(T)$ dependence for YbB_{12} is in good agreement with the data from previous work.¹⁵ Its main characteristic is a well-pronounced maximum at $T\approx 75$ K reflecting the formation of the nonmagnetic ground state. Substituting a moderate amount of Zr results in a clear change in this temperature dependence. The maximum is strongly smeared out and shifts toward higher temperatures, at variance with $\text{Yb}_{0.75}\text{Lu}_{0.25}\text{B}_{12}$, whose T dependence is indistinguishable from that of YbB_{12} above $T\sim 100$ K. From these results, one can expect the temperature dependence of the magnetic spectral response to be also less steep in $\text{Yb}_{0.8}\text{Zr}_{0.2}\text{B}_{12}$ than in YbB_{12} .

Figures 3(a)–3(d) present the magnetic excitation spectra of $\text{Yb}_{0.8}\text{Zr}_{0.2}\text{B}_{12}$ at four temperatures between 4.5 and 250 K, obtained by subtraction of the phonon background using the standard procedure described in Ref. 16. The spectra plotted for $T=4.5$ and 150 K combine data measured with $E_i=80$, 40, and 20 meV, yielding improved energy resolution (less than 1.5 meV full width at half maximum for the elastic line of a vanadium standard), similar to that achieved in the previous $\text{Yb}_{1-x}\text{Lu}_x\text{B}_{12}$ measurements. For comparison, the corresponding spectra for YbB_{12} and $\text{Yb}_{0.75}\text{Lu}_{0.25}\text{B}_{12}$ (Refs. 6 and 10) are shown in Figs. 3(e)–3(k).

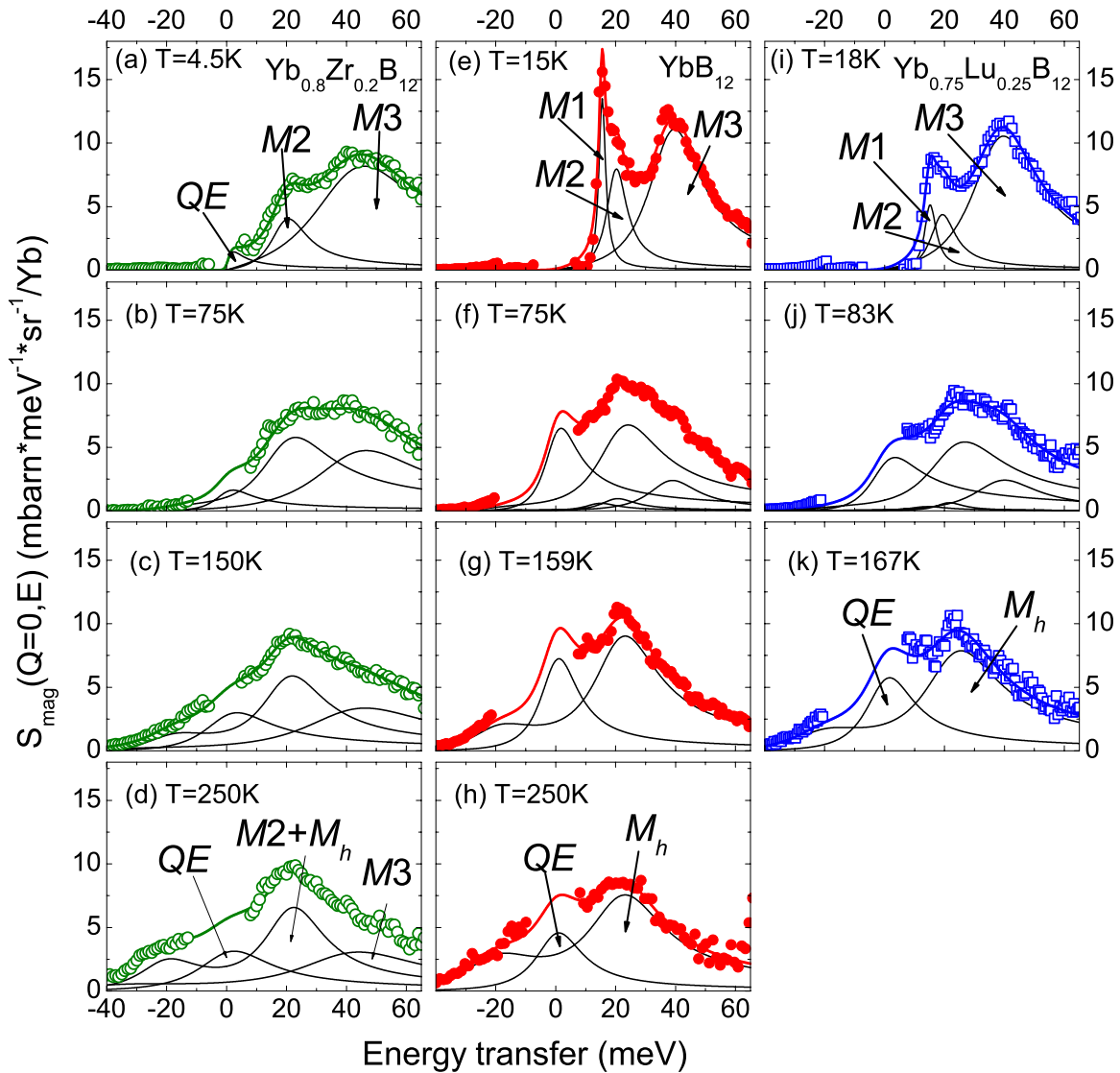


FIG. 3. (Color online) Magnetic excitation spectra of $\text{Yb}_{0.8}\text{Zr}_{0.2}\text{B}_{12}$ (this work, frames [a]–[d]), YbB_{12} and $\text{Yb}_{0.75}\text{Lu}_{0.25}\text{B}_{12}$ (from Refs. 6 and 10, frames [e]–[h] and [i]–[k], respectively) at temperatures between 4 and 250 K measured with incoming neutron energy $E_i = 80$ meV. (The spectra at $T=4.5$ K and $T=150$ K for $\text{Yb}_{0.8}\text{Zr}_{0.2}\text{B}_{12}$ and at $T=15$ K for YbB_{12} were in fact obtained by combining data measured with $E_i=80, 40$, and 20 meV). Symbols: experiments; lines: fit by Lorentzian spectral functions.

The effect of Zr substitution appears to be most pronounced at the lowest temperature, $T=4.5$ K. This effect is better seen on the expanded scale used in Fig. 4. In contrast to Lu substitution (also shown in Fig. 4), Zr doping results in the partial filling of the spin gap (0–15 meV) by a significant QE signal, with width $\Gamma/2 \sim 3$ meV, resulting in a pseudogap. This transformation is accompanied by the suppression of the in-gap excitation $M1$. The other peaks $M2$ and $M3$ are less affected, apart from some broadening. At high temperatures ($T=150$ and 250 K), the structure of the $\text{Yb}_{0.8}\text{Zr}_{0.2}\text{B}_{12}$ spectra also differs from that found in YbB_{12} . In particular, above 120 K, the YbB_{12} spectra consist of two components: a QE signal and the M_h peak whereas $\text{Yb}_{0.8}\text{Zr}_{0.2}\text{B}_{12}$ clearly exhibits an additional one at $E \sim 40$ meV [Figs. 3(c) and 3(d)], which could either be reminiscent of $M3$ or result from a new high-temperature excitation similar to M_h .

Following the previous analysis made for YbB_{12} ,⁷ one could try to interpret all three components of the high-temperature spectra (the QE signal and the two inelastic peaks) in terms of CF transitions. However, this is in contradiction with the temperature evolution of the magnetic spectra. According to Ref. 8, the CF level scheme in YbB_{12} consists of a Γ_8 quartet ground state and two quasidegenerate excited doublets Γ_7 and Γ_6 . To account for an extra peak occurring in the high-temperature spectrum of $\text{Yb}_{0.8}\text{Zr}_{0.2}\text{B}_{12}$, one has to suppose that the energy splitting between Γ_7 and Γ_6 states is enhanced. In this case, assuming a pure CF origin for the excitations at $T > 100$ K, increasing temperature should produce a decrease in the intensity of both inelastic peaks. In the present measurements, one instead sees some reduction in the 40 meV peak but accompanied by an *enhancement* of the 20 meV peak. This means that the origin of the peaks is different or that the crossover between low- and

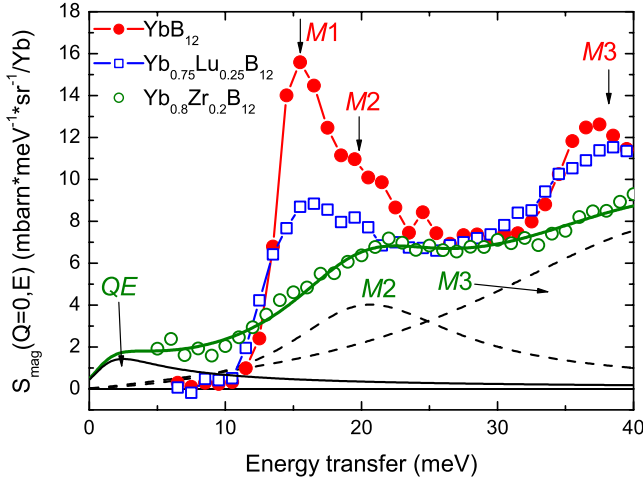


FIG. 4. (Color online) Low-temperature magnetic excitation spectra of YbB_{12} , $\text{Yb}_{0.75}\text{Lu}_{0.25}\text{B}_{12}$ (Refs. 6 and 10), and $\text{Yb}_{0.8}\text{Zr}_{0.2}\text{B}_{12}$ obtained by combining data measured with incoming neutron energy $E_i=80$, 40, and 20 meV. Symbols: experiments; lines: fit of the $\text{Yb}_{0.8}\text{Zr}_{0.2}\text{B}_{12}$ spectrum by Lorentzian spectral functions.

high-temperature regimes is not yet complete in the range of the measurements. A more consistent explanation would thus be that the peak observed near 40 meV still corresponds to the $M3$ excitation, which is not fully suppressed even at 250 K whereas the 20 meV peak contains, in addition to a residual signal from $M2$, a contribution from the $\Gamma_8 \rightarrow \Gamma_7/\Gamma_6$ CF transition. That the two excitations existing at high temperature may have different origins is further suggested by the fact that the 40 meV peak is almost twice as broad as the 20 meV peak.

In summary, the temperature evolution of the magnetic excitations in $\text{Yb}_{0.8}\text{Zr}_{0.2}\text{B}_{12}$ is qualitatively similar to that already reported for YbB_{12} but the transition from the low-temperature pseudogap regime to the high-temperature spin-fluctuation regime becomes much smoother with Zr substitution. The low-temperature excitations $M2$ and $M3$ are suppressed very slowly upon heating and persist up to the highest experimental temperature $T=250$ K. This, however, can be ascertained only from the variation in $M3$ because $M2$ cannot be distinguished from M_h in powder measurements. The behavior of $\text{Yb}_{0.8}\text{Zr}_{0.2}\text{B}_{12}$ turns out to be closer to the temperature dependence expected for the CF-split ground-state multiplet of a normal system with spin-orbit degeneracy than was the steep crossover observed in both YbB_{12} and $\text{Yb}_{1-x}\text{Lu}_x\text{B}_{12}$.

It was mentioned in Sec. I that the partial substitution of Yb by Lu does not destroy the local $f-d$ singlet because the main difference between the two elements is the absence of f -electron magnetic moment in Lu. In the case of Zr substitution, the difference is more drastic. In dodecaborides, Zr contributes *two* 4d electrons instead of *one* 5d in the case of Yb or Lu. Although the electron band structure in ZrB_{12} is similar to that of LuB_{12} ,^{17,18} one can assume that in a $\text{Yb}_{1-x}\text{Zr}_x\text{B}_{12}$ solid solution with moderate Zr concentration, the 4d electrons from zirconium do not populate the ytterbium 5d band but rather build up a separate 4d-impurity

band. If this is the case, Zr 4d electrons would not participate in the formation of the $f-d$ local bound state, leading to an incomplete “compensation” of the 4f magnetic moments by 5d electrons, in contrast to $\text{Yb}_{1-x}\text{Lu}_x\text{B}_{12}$. This could explain why experimentally the QE magnetic signal is found to exist in the $\text{Yb}_{1-x}\text{Zr}_x\text{B}_{12}$ spectra down to the lowest temperature. Interestingly, the depletion of compensating electrons at the Yb site can be regarded as causing a shift of the effective Yb valence toward 3+ (in undoped YbB_{12} it was previously determined¹⁹ to be equal to 2.95), which is also consistent with the contraction of the crystal lattice when Yb is replaced by Zr.

The behavior of $M1$, $M2$, and $M3$ appears to be in line with this picture. The existence of the spin exciton ($M1$) is closely related to the gaplike character of the spectrum and is not affected by moderate Lu dilution (Figs. 3 and 4). On the contrary, in the Zr-doped system the spin gap is partly filled and the gap edge is smeared out, causing the rapid suppression of $M1$. The other excitations $M2$ and $M3$, which have a different origin (reminiscent of CF states) and not very sensitive to the filling of the gap.

Another interesting effect of Zr dilution is the change in the temperature evolution of the dynamical spectral response. In $\text{Yb}_{1-x}\text{Lu}_x\text{B}_{12}$, as in undoped YbB_{12} , the magnetic spectra change rapidly with a moderate temperature increase, suggesting a steep crossover between low- and high-temperature regimes.⁸ Furthermore, the temperature at which this effect occurs is much lower than other characteristic energies of the system (Kondo temperature, gap value, and excitation energies).²⁰ This implies that the breakdown of the $f-d$ singlets in YbB_{12} and $\text{Yb}_{1-x}\text{Lu}_x\text{B}_{12}$ cannot be ascribed to a mere thermal depopulation of the ground state in a “rigid-band” picture but denotes a change in the nature of the electronic states. In $\text{Yb}_{0.8}\text{Zr}_{0.2}\text{B}_{12}$, the situation is qualitatively different. The spectra transform very smoothly with temperature and the low-temperature excitations $M2$ and $M3$ likely exist up to 250 K. The depletion of the 5d states due to Zr substitution thus appears to suppress the interaction responsible for the sharp crossover, leading to a more conventional temperature dependence. This smoother evolution, as well as the change from a true gap to a pseudogap, both contribute to smear out the maximum in the magnetic susceptibility (Fig. 2), which is characteristic for the Kondo insulator spin-gap state formation. The fact that the pseudogap regime extends to relatively high temperatures may also account for the higher resistivity values found in $\text{Yb}_{0.8}\text{Zr}_{0.2}\text{B}_{12}$.

More generally, the strong sensitivity of the ground state to Zr substitution strongly suggests that the formation of the local bound states involves the d states of the cation sites, rather than the boron p states, as was found previously in SmB_6 .²¹ Finally, one should keep in mind the sizable difference in masses (almost 50%) and ionic radii between Yb (or Lu) and Zr, which leaves open the possibility of alternative scenarios based on lattice (e.g., lattice distortion or magnetovibrational couplings) of chemical pressure effects.

IV. CONCLUSION

In present work, we have studied the spin dynamics in the new YbB_{12} -based solid solution $\text{Yb}_{1-x}\text{Zr}_x\text{B}_{12}$ ($x=0.2$). It was

found that the perturbation of the d -electron band due to the substitution of Zr for Yb affects the properties of the YbB_{12} Kondo insulator in a way that differs notably from that observed with Lu dilution. The $5d$ -electron band deficiency appears to hamper the local bound-state formation, which results in an incomplete quenching of the local $4f$ magnetic moment, as evidenced by the quasielastic magnetic signal seen in the INS spectrum at the lowest temperature. The transformation of the spin gap to a pseudogap in turn causes the suppression of the in-gap spin exciton ($M1$) at 15 meV.

These results emphasize the role of d -electron states in the formation of the singlet ground state. From this point of view, it would be of interest to study the spin dynamics of systems substituted by another $4d$ or even $3d$ element. One can expect that yttrium or scandium ions, despite being trivalent such as Lu, should produce effects similar to those of tetravalent zirconium.

The temperature dependence of the dynamical magnetic response becomes more conventional in $\text{Yb}_{0.8}\text{Zr}_{0.2}\text{B}_{12}$, in comparison with YbB_{12} , and is similar to that expected for a simple temperature dissociation of the f - d bound state. It can be concluded that the sharp temperature crossover in YbB_{12} , as well as its strong sensitivity to Zr substitution, are primarily connected with $5d$ -electron states, though an influence of lattice-related effects cannot be ruled out.

ACKNOWLEDGMENTS

We are grateful to L. A. Maksimov, A. F. Barabanov, P. Thalmeier, L.-P. Regnault, and Ph. Bourges for stimulating discussions. The work was supported by the RFBR under Grant No. 08-02-00430.

-
- ¹P. S. Riseborough, *Adv. Phys.* **49**, 257 (2000).
²F. Iga, N. Shimizu, and T. Takabatake, *J. Magn. Magn. Mater.* **177-181**, 337 (1998).
³J. Otsuki, *J. Phys. Soc. Jpn.* **76**, 064707 (2007).
⁴A. Akbari, P. Thalmeier, and P. Fulde, *Phys. Rev. Lett.* **102**, 106402 (2009).
⁵A. F. Barabanov and L. A. Maksimov, *Phys. Lett. A* **373**, 1787 (2009).
⁶E. V. Nefeodova, P. A. Alekseev, J.-M. Mignot, V. N. Lazukov, I. P. Sadikov, Yu. B. Paderno, N. Yu. Shitsevalova, and R. S. Eccleston, *Phys. Rev. B* **60**, 13507 (1999).
⁷J.-M. Mignot, P. A. Alekseev, K. S. Nemkovski, L.-P. Regnault, F. Iga, and T. Takabatake, *Phys. Rev. Lett.* **94**, 247204 (2005).
⁸K. S. Nemkovski, J.-M. Mignot, P. A. Alekseev, A. S. Ivanov, E. V. Nefeodova, A. V. Rybina, L.-P. Regnault, F. Iga, and T. Takabatake, *Phys. Rev. Lett.* **99**, 137204 (2007).
⁹G. Aeppli and Z. Fisk, *Comments Condens. Matter Phys.* **16**, 155 (1992).
¹⁰P. A. Alekseev, J.-M. Mignot, K. S. Nemkovski, E. V. Nefeodova, N. Yu. Shitsevalova, Yu. B. Paderno, R. I. Bewley, R. S. Eccleston, E. S. Clementyev, V. N. Lazukov, I. P. Sadikov, and N. N. Tiden, *J. Phys.: Condens. Matter* **16**, 2631 (2004).
¹¹J.-M. Mignot, P. A. Alekseev, K. S. Nemkovski, E. V. Nefeodova, A. V. Rybina, L.-P. Regnault, N. Yu. Shitsevalova, F. Iga, and T. Takabatake, *Physica B* **383**, 16 (2006).
¹²T. Kasuya, *J. Phys. Soc. Jpn.* **65**, 2548 (1996).
¹³S. H. Liu, *Phys. Rev. B* **63**, 115108 (2001).
¹⁴F. Iga, T. Suemitsu, S. Hiura, K. Takagi, K. Umeo, M. Sera, and T. Takabatake, *J. Magn. Magn. Mater.* **226-230**, 137 (2001).
¹⁵F. Iga, S. Hiura, J. Klijn, N. Shimizu, T. Takabatake, M. Ito, Y. Matsumoto, F. Masaki, T. Suzuki, and T. Fujita, *Physica B* **259-261**, 312 (1999).
¹⁶A. P. Murani, *Phys. Rev. B* **50**, 9882 (1994).
¹⁷I. R. Shein and A. L. Ivanovskii, *Phys. Solid State* **45**, 1429 (2003).
¹⁸G. E. Grechnev, A. E. Baranovskiy, V. D. Fil, T. V. Ignatova, I. G. Kolobov, A. V. Logosha, N. Yu. Shitsevalova, V. B. Filipov, and O. Eriksson, *Low Temp. Phys.* **34**, 921 (2008).
¹⁹P. A. Alekseev, E. V. Nefeodova, U. Staub, J.-M. Mignot, V. N. Lazukov, I. P. Sadikov, L. Soderholm, S. R. Wassermann, Yu. B. Paderno, N. Yu. Shitsevalova, and A. Murani, *Phys. Rev. B* **63**, 064411 (2001).
²⁰A. Bouvet, Ph.D thesis, University of Grenoble, 1993.
²¹K. A. Kikoin and A. S. Mishchenko, *J. Phys.: Condens. Matter* **7**, 307 (1995).